

Chemical Modification of the Rieske Protein from *Thermus thermophilus* Using Diethyl Pyrocarbonate Modifies Ligating Histidine 154 and Reduces the [2Fe-2S] Cluster[†]

Mary E. Konkle,[‡] Kaitlin N. Elsenheimer,[‡] Kevin Hakala,[§] Jennifer C. Robicheaux,[‡]
Susan T. Weintraub,[§] and Laura M. Hunsicker-Wang^{*,‡}

[‡]Department of Chemistry, Trinity University, One Trinity Place, San Antonio, Texas 78212, and [§]Department of Biochemistry and Mass Spectrometry Core Laboratory, University of Texas Health Science Center at San Antonio, San Antonio, Texas 78229

Received May 18, 2010; Revised Manuscript Received July 19, 2010

ABSTRACT: Rieske proteins are a class of electron transport proteins that are intricately involved in respiratory and photosynthetic processes. One unique property of Rieske proteins is that the reduction potential is pH-dependent. The ionizable groups responding to changes in pH have recently been shown to be the two histidine residues that ligate the [2Fe-2S] cluster. To probe the chemical reactivity toward and the accessibility of the ligating histidines to small molecules, akin to the substrate quinol and the inhibitor stigmatellin, the *Thermus thermophilus* Rieske protein was reacted with diethyl pyrocarbonate (DEPC) over a range of pH values. The modification was followed by UV–visible, circular dichroism, and EPR spectroscopies and the end product analyzed by mass spectrometry. The ligating His154, as well as the two nonligating histidines and surface-exposed lysines, were modified. Interestingly, modification of the protein by DEPC was also found to reduce the metal cluster. The ability to control the redox state was examined by the addition of oxidants and reductants and removal of the DEPC–histidine adduct by sodium hydroxide. Characterization of the DEPC-modified Rieske protein, which remains redox active, offers a probe to analyze the effects of small molecules that inhibit the function of the *bc*₁ complex and that have also been shown to interact with the ligating histidines of the Rieske [2Fe-2S] cluster in crystal structures of the complex.

Rieske proteins are electron transport proteins that are involved in key biological processes such as cellular respiration (as part of the *bc*₁ complex) and photosynthesis (as part of the *b₆f* complex) (1, 2). The redox-reactive component of the Rieske protein is a [2Fe-2S] cluster that is ligated by two cysteine and two histidine residues which are the only strictly conserved residues across the Rieske and Rieske-type family (3). All Rieske proteins, including the soluble portion of the Rieske protein from *Thermus thermophilus* (trunc*TiRp*)¹ utilized in this study, have been shown to have pH-dependent reduction potentials (4, 5), with the histidines ligating to the cluster deprotonating in response to increases in pH (6).

Diethyl pyrocarbonate (DEPC) is a widely used chemical modifier that reacts with deprotonated histidines to transfer a carbethoxy

moiety (C(O)OCH₂CH₃) onto the ring nitrogen (Figure 1b) (7). In addition, it reacts with side chains of lysines and tyrosines and the protein N-terminus. Many studies over the years have used this reagent as a probe to determine whether a catalytic mechanism involves a critical histidine, as indicated by disruption of enzymatic action after formation of a DEPC–histidine adduct (8). DEPC has been shown to inhibit the *bc*₁ complex, and preliminary studies suggested that the mechanism of inhibition is through formation of a functionally inert adduct of the Rieske protein. A possible mechanism of inhibition is modification of the histidines ligating to the [2Fe-2S] cluster (9–12).

The importance of the ligating histidines can be examined, in part, by analyzing their interactions with small molecule inhibitors of the *bc*₁ complex. There are numerous crystal structures of the complete *bc*₁ complex (43 total) from several different organisms which also have small molecules bound in the active site of those structures (13–28). Stigmatellin has been used as a small molecule probe of the quinol binding site in numerous crystallographic studies and has been shown to interact with the Rieske protein via a hydrogen bond to the N ϵ of the higher numbered ligating histidine residue (13–18, 21–25). Stigmatellin was originally reported in 1985 to be an inhibitor of the *bc*₁ complex (29) and was subsequently shown to inhibit movement of the Rieske protein between quinol and cytochrome *c*₁ (13). A more recent study suggested that the mechanism of inhibition also involves the reduction of the [2Fe-2S] complex of the Rieske protein. The source of electron in this process, however, is unknown (30). Additionally, it has been hypothesized that *bc*₁ complex inhibition by other xenobiotics, such as chromonols and ascochlorin, is also through, at least in part, interaction with the ligating histidine(s) of the Rieske protein (31, 32). The degree to which these small

[†]This work was supported by the Welch Foundation [W-1661 (to L.M.H.-W.), W-0031 (Trinity Chemistry Department)], and Research Corporation (Cottrell College Science Award 7963). Acknowledgment is made to the Donors of the American Chemical Society Petroleum Research Fund for partial support of this research. The CD was acquired and supported by the National Science Foundation (BIO MRI-0718766). K.N.E. was supported in part by a research fellowship provided by Trinity University. J.C.R. was supported by a research fellowship through the Howard Hughes Medical Institute.

*To whom correspondence should be addressed: e-mail, laura.hunsickerwang@trinity.edu; phone, (210) 999-7895; fax, (210) 999-7569.

¹Abbreviations: trunc*TiRp*, *Thermus thermophilus* Rieske protein previously characterized; H120Q/H162Q, trunc*TiRp* with mutations of histidine to glutamine at positions 120 and 162; *bc*₁ complex, complex III of the respiratory chain/quinol:cytochrome *c* oxidoreductase; DEPC, diethyl pyrocarbonate; DMSO, dimethyl sulfoxide; MES, 2-(*N*-morpholino)ethanesulfonic acid hydrate; MOPS, 3-(*N*-morpholino)propanesulfonic acid; TFA, trifluoroacetic acid; Tris, 2-amino-2-(hydroxymethyl)-1,3-propanediol; IPTG, isopropyl β -D-1-thiogalactopyranoside; TCEP, tris(2-carboxyethyl)phosphine; EDTA, ethylenediaminetetraacetic acid; HAc, acetic acid; CD, circular dichroism; EPR, electron paramagnetic resonance; LMCT, ligand to metal charge transfer; CID, collision induced decay.

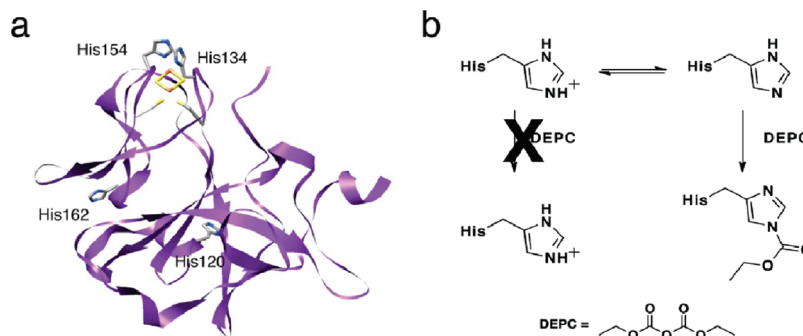


FIGURE 1: (a) Crystal structure of truncTtRp (PDB code 3FOU) in ribbon representation (purple). The [2Fe-2S] cluster, histidines, and ligating residues are shown as sticks in color by atom. (b) Scheme, based on the figure in ref 7, of the reaction of DEPC with deprotonated histidines.

molecule–protein interactions influence the electronics of the [2Fe-2S] cluster, however, has yet to be fully characterized.

The Rieske protein from *T. thermophilus* has been reported to have two pK_a values for the oxidized protein, $pK_{ox1} = 7.8$ and $pK_{ox2} = 9.6$, and one pK_a for the reduced protein, $pK_{red} = 12.5$ (4). An additional role for the histidine ligands, substantiated by spectroscopic measurements and theoretical calculations, is that these pK_a values reflect the protonation/deprotonation of the N ϵ atoms of the two ligating histidines and, thus, are responsible for the pH-dependent reduction potential (33–37). A recent study showed pH-dependent ^{15}N NMR shifts for His134 and His154 of the *T. thermophilus* Rieske and assigned the lower pK_a to His154 (6). Thus, the pK_{a2} of the ligated histidines is lowered from the expected pK_{a2} of 14.5 due to ligation to the [2Fe-2S] center. Clarifying the reactivity of the histidines ligated to the [2Fe-2S] cluster is critical for elucidating the available types of molecular interactions with the intended redox partners (quinol and cytochrome *c*, or their equivalents), small molecule inhibitors, or protein/protein interactions within the complete *bc*₁ complex.

In this study, DEPC was used to modify the protein in order to gain insight into the reactivity of the histidines and to probe the effects of chemical modification of the ligating histidine(s) on the redox state of the [2Fe-2S] cluster. We used DEPC to trap the deprotonated ligating histidine(s). UV–visible, circular dichroism (CD), and electron paramagnetic resonance (EPR) spectroscopies were utilized to monitor the effect(s) of this modification on the electronics and structure near the metal center. Subsequently, mass spectrometry analysis definitively identified the ligating His154, among other residues, as being modified by DEPC. Chemical modification of the Rieske protein from *T. thermophilus* by DEPC affords a way to examine the reactivity of the ligand histidines of Rieske proteins and provides insight into how the interactions of the ligating histidine residues influence the protein's redox properties.

MATERIALS AND METHODS

Mutagenesis and Expression of Rieske Protein. The vector used for expression of truncTtRp, which lacks 17 residues found in TtRp, is the construct previously described (37). Mutagenesis of the histidine residues in the large domain (His120 and His162) was accomplished in sequential PCR reactions using the Strategene QuikChange kit (Agilent Technologies, La Jolla, CA) supplemented with 5 μL of GC-Melt buffer (Clontech, Mountain View, CA) and 2.5 μL of DMSO to the 50 μL reaction. The following primers were used: 5'-GAGGTGGCCAGCAAGCCG-CGGAGGGC-3' for H120Q and 5'-GTACGACCTCAGG-CAAGGCGCCAGGTC-3' for H162Q. The plasmid containing

the gene for truncTtRp and His120Gln/His162Gln truncTtRp (H120Q/H162Q) in the multiple cloning site was transformed into C41(DE3) competent cells (Lucigen Corp., Middleton, WI) according to the manufacturer's protocol. The transformed cells were grown on YT plates and in TB broth in the presence of ampicillin (100 $\mu\text{g}/\text{mL}$). A 6 L culture was grown and induced with 0.4 mM IPTG when the $\text{OD}_{600} = 1$ AU. Supplements, 150 μM cysteine and 150 $\mu\text{g}/\text{mL}$ ferric ammonium citrate (final concentration), were added to the cultures upon induction to aid in the synthesis of the [2Fe-2S] cluster. The cells were harvested and lysed as described previously (37). The lysate was dialyzed into 50 mM Tris, pH 8.0. All subsequent steps in the isolation proceeded as previously described except that the ammonium sulfate precipitation step was not used. Removal of this step increased the yields of isolated protein. All isolated proteins were in the oxidized state and were found to be stable. The purity of each protein was assessed by SDS–PAGE. The concentration of each protein was determined by the difference in AU_{572} of the isolated oxidized form and the reduced form obtained by the addition of an excess of sodium dithionite (37). The expression of H120Q/H162Q (4.3 mg/L of culture) was lower than that of truncTtRp (20 mg/L of culture). The addition of iron- and sulfur-containing supplements at induction increased the expression of H120Q/H162Q 9-fold.

DEPC Modification Monitored by UV–Visible Spectrophotometry. All UV–visible data were collected on a Hitachi U-3000 spectrophotometer (Chicago, IL) with a 1 cm path length in quartz microcuvettes. The experimental conditions used were as follows: scan speed 600 nm/min; slit 2 nm; cycle time 2 min. The purified proteins were stored in 25 mM Tris buffer with 100 mM NaCl at pH 8.0. Prior to the modification experiments, the proteins were dialyzed to exchange the Tris buffer (which readily reacts with DEPC) into 25 mM buffer at the desired pH (see below). The buffers used at the various pH conditions were as follows: pH 6, MES buffer; pH 7, MOPS buffer; pH 8 and 9, sodium phosphate. The pH was checked after dialysis and before modification to ensure that no drift had occurred. The samples were diluted to 0.5 mL (48 μM), and UV–visible spectroscopy (650–230 nm) was used to monitor the modification after the addition of DEPC (5 μL , neat) at 2 min intervals over 24 min. The experiments were performed in triplicate, and the data were processed as difference spectra by subtracting the spectrum of the protein prior to the addition of DEPC from each spectrum taken after DEPC addition.

DEPC Modification Monitored by Circular Dichroism. CD spectra were collected on a Jasco J-815 spectropolarimeter (Tokyo, Japan). Experimental conditions used for single scans

were as follows: bandwidth, 2 nm; scan speed, 500 nm/min; resolution, 1 nm; temperature, 25 °C; response time, 1 s. The purified protein was diluted to a final concentration of 100 μ M in a final volume of 400 μ L of 25 mM buffer appropriate for the desired pH for spectra collected from 650 to 230 nm and 34.5 μ M for the spectra taken at 260–200 nm. For the spectral comparison of reduced and oxidized trunc*Tt*Rp and H120Q/H162Q, the protein concentrations were 138 μ M in 20 mM Tris, pH 8.0, and 100 mM NaCl. All chemicals used were obtained from Sigma Aldrich Chemical Co. (St. Louis, MO). Prior to analysis, the purified proteins were dialyzed into 25 mM buffer at the desired pH according to the protocols above. CD (650–230 nm) was used to monitor the modification by DEPC (5 μ L, neat) at 2 min intervals over 90 min at various pH values from 6.0 to 9.0. All experiments were performed in triplicate at 25 °C.

Oxidation/Reduction of DEPC-Modified H120Q/H162Q. Immediately after modification of H120Q/H162Q, the sample was treated with potassium ferricyanide (1 mM) or sodium dithionite (10 mM). The change in oxidation state of the modified protein was monitored with CD (650–230 nm) at 2 min intervals over 20 min.

EPR of the DEPC-Modified Proteins. Trunc*Tt*Rp and H120Q/H162Q were modified with DEPC as described above. For the ferricyanide experiment, 10 mM potassium ferricyanide was added to the sample after the 90 min reaction with DEPC. The samples were then dialyzed and concentrated to a final protein concentration of 900 μ M after being cryoprotected with 30% (v/v) glycerol. The samples were frozen at –80 °C. EPR spectra were acquired at the CalEPR center at the University of California, Davis, on a Bruker ECS 106 continuous wave X-band spectrometer. Data were collected at 10 K in an Oxford ESR 900 liquid helium cryostat using an Oxford ITC503 temperature controller. Field calibration was done at room temperature using *g*-value marker LiF:Li (*g* = 2.002293).

Removal of DEPC Adducts of Histidine(s). Immediately after DEPC modification of H120Q/H162Q using CD, 5 μ L of 9 M sodium hydroxide (final concentration of 150 mM) was added to the sample. The removal of the DEPC adduct from the histidine was monitored by CD (650–230 nm) and UV–visible (600–230) spectroscopies at 2 min intervals over 40 min. Additionally, a control sample of the same pH and concentration (no DEPC added) of H120Q/H162Q was treated with an equal amount of sodium hydroxide and characterized by CD to account for any effect of pH on the spectrum.

Mass Spectrometry. After modification of trunc*Tt*Rp or H120Q/H162Q with DEPC, the protein was dialyzed into 20 mM ammonium bicarbonate. The protein was diluted 1:1 into 0.2% trifluoroacetic acid (TFA) and applied to a C₄ ZipTip (Millipore, Billerica, MA). The protein was subsequently eluted from the ZipTip by 50 μ L of 50% acetonitrile containing 0.2% TFA and dried by vacuum centrifugation (SpeedVac; Thermo Fisher Scientific, Waltham, MA). Proteolytic digestion was accomplished by addition of 20 ng of chymotrypsin (Sigma Chemical Co.) in 10 μ L of 40 mM ammonium bicarbonate, pH 8, containing 10% acetonitrile, 5 mM TCEP, and 5 mM EDTA to the dried sample to give an enzyme:protein ratio of ~20:1. The digestion was allowed to proceed overnight at 30 °C. The digests were analyzed by capillary HPLC–electrospray ionization–tandem mass spectrometry (HPLC–ESI–MS/MS) using a Thermo Fisher LTQ linear ion trap mass spectrometer fitted with a New Objective PicoView 550 nanospray interface. Online HPLC separation was accomplished with an Eksigent NanoLC micro HPLC:

column, PicoFrit (New Objective; 75 μ m i.d.) packed to 11 cm with C18 adsorbent (Vydac; 218MSB5, 5 μ m, 300 Å); mobile phase A, 0.5% acetic acid (HAc)/0.005% TFA; mobile phase B, 90% acetonitrile/0.5% HAc/0.005% TFA; gradient, 2–42% B in 30 min; flow rate, 0.4 μ L/min. MS conditions were as follows: ESI voltage, 2.9 kV; isolation window for MS/MS, 3; relative collision energy, 35%; scan strategy, survey scan followed by acquisition of data-dependent collision-induced dissociation (CID) spectra of the seven most intense ions in the survey scan above a set threshold. The uninterpreted CID spectra were searched by means of Mascot (Matrix Science, London, U.K.) against a database that contains the sequences of the expressed proteins concatenated to the Swiss-Prot database. Chymotrypsin was specified as the proteolytic enzyme, and three missed cleavages were allowed. Variable modifications considered were DEPC modification of histidine and lysine and oxidation of methionine and proline. Peak lists were created using extract_msn.exe. Precursor and fragment ion mass tolerances were ± 1.5 and ± 0.8 Da, respectively. Cross-correlation of the Mascot results with X! Tandem and determination of protein identity probabilities were accomplished by Scaffold (Proteome Software, Portland, OR).

RESULTS

To investigate the reactivity of the ligand histidines that are involved in the pH-dependent reduction potential, Rieske proteins from *T. thermophilus* (Figure 1a) were reacted with DEPC. When DEPC reacts with histidines, it only modifies deprotonated histidines (Figure 1b) to form a covalent carbethoxy–histidine adduct. Trunc*Tt*Rp contains a total of four histidine residues (Figure 1a), two of which are ligated to the [2Fe–2S] cluster (His134 and His154) and are strictly conserved across isoforms. The remaining two histidines (His120 and His162) are not spatially close to the metal cluster and are not conserved across isoforms. A double mutant, H120Q/H162Q, was designed to provide a protein in which each nonligating histidine was mutated to glutamine. Thus, only the ligand histidines remained. The mutant was produced and purified in order to directly probe the roles of the conserved histidine residues ligated to the redox-active [2Fe–2S] cluster.

Spectroscopic Characterization of H120Q/H162Q. To ensure that the mutagenesis to H120/H162Q did not fundamentally alter the protein structure, the protein fold was assessed by CD (260–200 nm) in the amide backbone region and compared to trunc*Tt*Rp. The oxidized and chemically reduced forms (using excess dithionite) of trunc*Tt*Rp and H120Q/H162Q were compared using CD and are nearly identical (Supporting Information Figure S1). The *pK_a* values of the oxidized H120Q/H162Q protein were determined by fitting the change in AU₄₃₆ as a function of pH using UV–visible spectroscopy, as previously described (37). The *pK_{ox1}* = 7.29 \pm 0.15 and *pK_{ox2}* = 9.69 \pm 0.10 for H120Q/H162Q are similar to trunc*Tt*Rp (Supporting Information Figure S1) (37). Thus, trunc*Tt*Rp and H120Q/H162Q were considered to be sufficiently identical in structural and biophysical characteristics to be used for the current study.

Monitoring DEPC Modification by UV–Visible Spectroscopy. Modification of histidine with DEPC occurs only when the imidazole side chain of the histidine is deprotonated (Figure 1b) (7). As such, this modification is a particularly useful tool to probe the protonation state of histidine residues. The extent of modification of trunc*Tt*Rp and H120Q/H162Q by DEPC was initially determined by UV–visible spectroscopy using the characteristic absorbance of the carbethoxy–histidine chromophore at 240 nm (7).

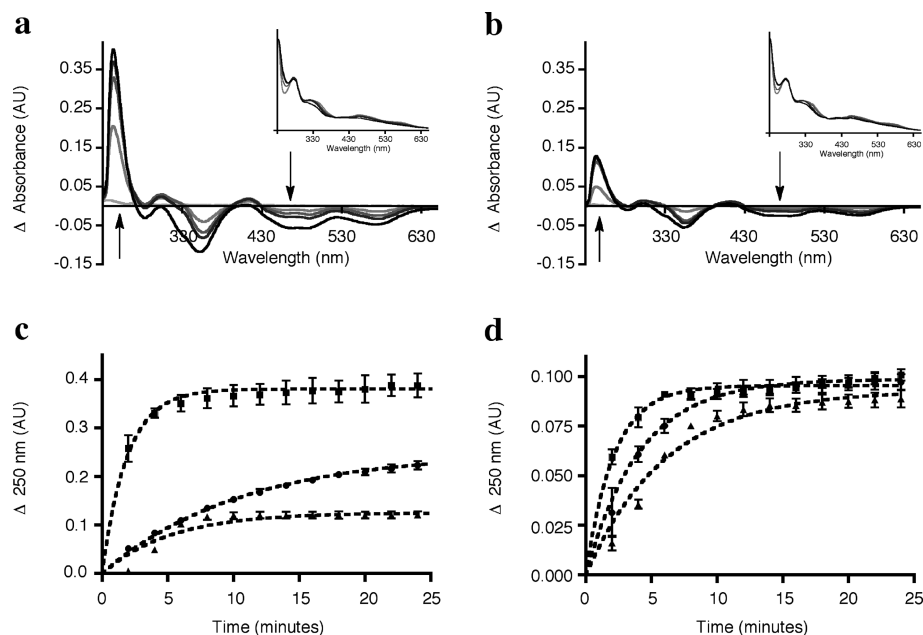


FIGURE 2: Treatment of (a) truncTtRp and (b) H120Q/H162Q modified at pH 8.0 by DEPC as analyzed by UV–visible difference spectra (650–230 nm) of time points taken 2, 4, 6, and 18 min after the addition of DEPC. Arrows denote the increase at 250 nm due to the accumulation of the DEPC–histidine adduct and the decrease in the LMCT bands. Insets: Raw data before subtraction. Plot of change at 250 nm of treatment of (c) truncTtRp and (d) H120Q/H162Q by DEPC at pH 6.0 (triangles), 7.0 (circles), and 8.0 (squares). Dotted lines are shown for depiction only. Error bars shown are SEM of triplicate measurements.

Upon addition of DEPC to both truncTtRp and H120Q/H162Q, the absorbance increased maximally at 250 nm² and was monitored over time (panels a and b of Figure 2, respectively) in order to confirm that DEPC–histidine adducts were forming. Detection of the chromophore in the DEPC adduct of the H120Q/H162Q mutant (which contains only the two ligating histidines) indicated that at least one of the ligands had been modified.

DEPC modification was performed at pH 6.0, 7.0, 8.0, and 9.0 for both truncTtRp and H120Q/H162Q. For pH 6–8, the rate of modification, as determined by the time needed to reach maximum change in absorbance at 250 nm ($\Delta 250_{\text{max}}$), increased with increasing pH for both proteins (Figure 2c,d); $\Delta 250_{\text{max}}$ was achieved by 24 min for all pH values. Using the published molar absorptivity of 3200 M^{−1} cm^{−1} for the chromophore at 240 nm (7), with the caveat that the maximum in this study is actually at 250 nm, the number of modified histidines for truncTtRp can be estimated, and it increases from 0.8 to 1.6 to 2.5 for pH 6–8, respectively (Table 1). The behavior of both truncTtRp and H120Q/H162Q at pH 9.0 was slightly different than for pH 6–8 (see below).

Interestingly, the extent of modification, as defined by $\Delta 250_{\text{max}}$, was only pH-dependent for truncTtRp and not for H120Q/H162Q. $\Delta 250_{\text{max}}$ for DEPC modification of H120Q/H162Q was less than that of truncTtRp, consistent with removal of 50% of the histidines by mutagenesis. In addition, estimating the number of modified histidines indicates that only 0.6–0.7 histidines are modified at pH 6–9 (Table 1). These results indicate that there is only one histidine that is modified in H120Q/H162Q.

TruncTtRp behaved differently when modified by DEPC at pH 9.0 compared to pH 6–8. The extent of modification ($\Delta 250_{\text{max}}$)

Table 1: Extent of DEPC Modification of truncTtRp and H120Q/H162Q

pH	$\Delta 250_{\text{max}}$, nm (AU) ^a		estimated no. of modified histidines ^b	
	truncTtRp	H120Q/H162Q	truncTtRp	H120Q/H162Q
6.0	0.125 ± 0.003	0.381 ± 0.006	0.8 ± 0.02	0.6 ± 0.04
7.0	0.092 ± 0.003	0.098 ± 0.002	1.6 ± 0.02	0.7 ± 0.01
8.0	0.250 ± 0.004	0.127 ± 0.009	2.4 ± 0.03	0.6 ± 0.06
9.0	0.112 ± 0.005	0.095 ± 0.001	0.8 ± 0.03	0.6 ± 0.01

^a $\Delta 250_{\text{max}}$ nm is calculated as the maximum difference at 250 nm, with the reported value as the average ± the standard deviation of the three runs. ^bThese numbers represent an estimation of the number of modified histidines using the molar absorptivity of 3200 M^{−1} cm^{−1} at 240 nm. These values come from the maximum at 250 nm (see footnote 2).

at pH 9.0 was less than that at pH 8.0 (Table 1). This result can be explained by the reversibility of the carboxy–histidine at alkaline pH (7). Estimating the number of modified histidines gives 0.8 histidines modified at pH 9. These data are consistent with at least one histidine in truncTtRp that was modified by DEPC retaining the adduct at this pH. In contrast, there was no loss of the histidine–DEPC chromophore of modified H120Q/H162Q at pH 9.0. One interpretation is that the ligating histidine residue(s) modified by DEPC is stable at pH 9.0. However, the nonligating histidine residues (present in truncTtRp but not in H120Q/H162Q) that are modified by DEPC are not stable at high pH.

While the observed increase in absorbance at 250 nm confirmed the successful modification of histidines by DEPC in both truncTtRp and H120Q/H162Q, the histidine–DEPC chromophore is not able to discriminate between ligating and nonligating histidines. To examine the effects of DEPC modification on the metal center, the three major LMCT bands in the oxidized truncTtRp protein (325, 458, and 560 nm) were analyzed. Concurrent to the increase in the absorbance at 250 nm, a decrease in the LMCT bands in the visible region (600–300 nm) was observed

²The chromophore of the histidine–DEPC adducts of the Rieske protein are red shifted from the canonical 240 to 250 nm. Additionally, the ligation of either 50% (truncTtRp) or 100% (H120Q/H162Q) of the available histidines to the [2Fe-2S] cluster would inevitably affect the molar absorptivity of the ligated residues. The calculated values represent, therefore, an estimate of the number of modified histidines.

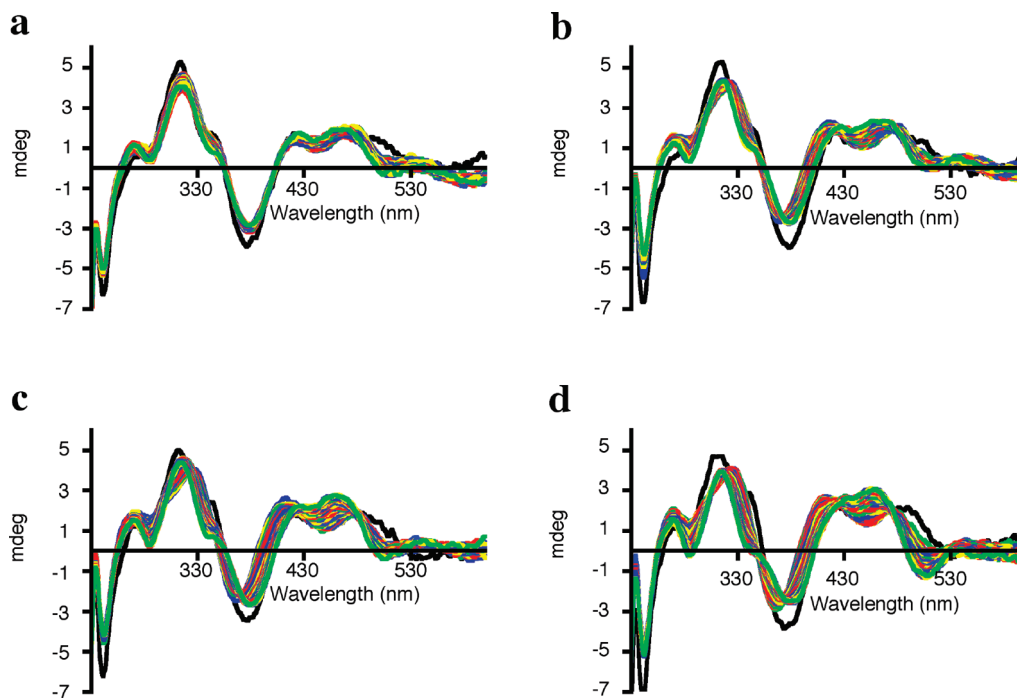


FIGURE 3: Modification of H120Q/H162Q by DEPC as monitored by CD (600–230 nm) at pH (a) 6.0, (b) 7.0, (c) 8.0, and (d) 9.0. The spectra were taken at 2 min intervals over 90 min. The initial spectrum is in black, and the final spectrum is in green.

upon addition of DEPC (Figure 2a). The decrease in the LMCT bands became more pronounced at higher pH. There was also a blue shift of the 325 nm LMCT band upon DEPC modification that became evident at higher pH (Figure 2a, inset). The changes in the LMCT bands resulting from DEPC modification were only slightly different between trunc*TtRp* and H120Q/H162Q (Figure 2a,b). The similarity in changes to the LMCT bands between the two proteins provides compelling evidence that the reaction with DEPC produced modified histidines that are ligands to the cluster since H120Q/H162Q contains only the two ligand histidines.

Monitoring DEPC Modification by CD Spectroscopy. CD spectroscopy is an especially useful tool for the current study because the presence of the [2Fe-2S] cluster gives a strong spectroscopic signature in the visible region. Modification of H120Q/H162Q using an excess of DEPC was performed at different pH values (6.0, 7.0, 8.0, 9.0) and monitored using CD (600–230 nm) for 90 min after the addition of excess DEPC (Figure 3). A complex set of changes at 315, 340, 385, 400, 450, and 500 nm resulted from DEPC modification; the extent of change in these signals was more pronounced with higher pH (Figure 3). No significant alteration of the global fold was observed after DEPC modification (Supporting Information Figure S2). Additionally, no loss of signal originating from the metal center was observed, indicating that the protein remained predominantly in *holo* form. Modification of trunc*TtRp* by DEPC in various pH environments resulted in similar changes as H120Q/H162Q (Supporting Information Figure S3). Taken together, these results substantiate the conclusion that the altered spectroscopic signals in the visible region derive from the common histidines in the two proteins, the ligands to the [2Fe-2S] cluster.

Removal of DEPC–Histidine Adduct(s). Histidine modification by DEPC is reversible by treatment with hydroxylamine or alkaline pH (7). The ability to remove the DEPC adduct from histidine is particularly useful to differentiate between the reversible reactions of DEPC with histidine from the irreversible, nonspecific

reactions with lysine or tyrosine residues. H120Q/H162Q was reacted with DEPC at pH 8.0 as described above. After the modification reaction, concentrated sodium hydroxide was added, and the time course of removal of the DEPC from histidine was monitored by UV–visible and CD spectroscopies (Figure 4). A matched control sample, also at pH 8, was treated with the same amount of sodium hydroxide. The final spectrum of sodium hydroxide-treated, modified protein was nearly identical to untreated protein at the same pH, indicating that removal of the DEPC adduct from the ligating histidine residue(s) restored the [2Fe-2S] cluster to its native state (Figure 4b). The removal of the DEPC adducts on histidine by sodium hydroxide also restored the LMCT bands, concurrent with the loss of the 250 nm chromophore (Figure 4a), further confirming that the H120Q/H162Q is still in the *holo* form after modification and that the changes induced by DEPC modification are reversible. Protein treated in this way can still be reduced with dithionite (data not shown).

Mass Spectrometry Analysis of DEPC-Modified Proteins. The modification of histidine residues by DEPC is readily detectable in the UV–visible spectrum due to the characteristic carboxy–histidine chromophore, but the adducts with tyrosines and lysines are not readily observed by spectroscopy since they do not produce new chromophores. However, it is possible to fully characterize the end product(s) to determine the specific location of the chemical modifications on the proteins through use of tandem mass spectrometry. Trunc*TtRp* and H120Q/H162Q modified with DEPC at pH 7.6 were proteolytically digested with chymotrypsin and analyzed by HPLC–electrospray tandem mass spectrometry. The sequence information provided by the tandem mass spectra permitted unambiguous identification of the modified residues which exhibited the expected mass shifts due to addition of +72 Da per carboxy group.

After chymotryptic digestion, all four of the histidine residues of trunc*TtRp* were detected, each in a separate peptide. Ligating His154 was found as DEPC-modified and unmodified states in

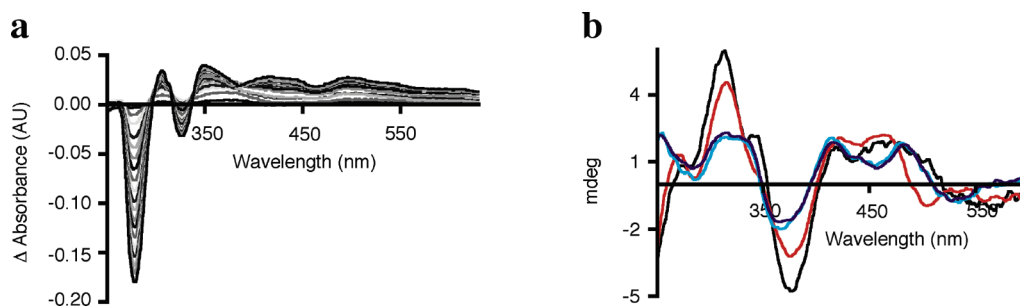


FIGURE 4: Removal of the carboxy-histidine adduct of H120Q/H162Q by treatment with sodium hydroxide monitored by (a) UV-visible difference spectra of time points taken every 2 min after the addition of sodium hydroxide. The difference is the DEPC-modified protein subtracted from DEPC-modified protein with sodium hydroxide. The final spectrum is in black. (b) CD spectra of H120Q/H162Q (black), DEPC-modified H120Q/H162Q (red), sodium hydroxide-treated DEPC-modified H120Q/H162Q (cyan), and sodium hydroxide-treated H120Q/H162Q (purple).

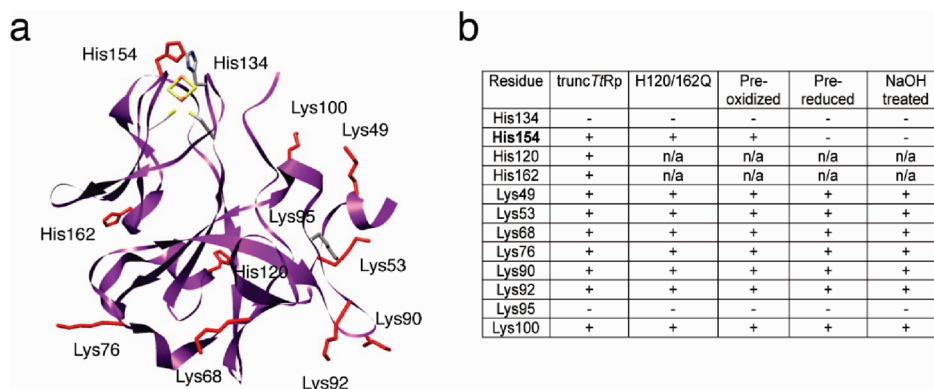


FIGURE 5: Mass spectrometry analysis of truncTfRp and H120Q/H162Q treated with DEPC under various conditions. (a) Representation of all histidine and lysine (PDB code 3FOU, ribbon in purple) with the residues that have been observed in the DEPC-modified state shown in sticks and colored in red. Residues pictured in color by atom are not observed as DEPC-modified. (b) Chart showing the state of modification by DEPC in truncTfRp (column 1), H120Q/H162Q (column 2), “preoxidized” H120Q/H162Q treated with DEPC (column 3), “prereduced” H120Q/H162Q treated with DEPC (column 4), and DEPC-modified H120Q/H162Q subsequently treated with sodium hydroxide (column 5). The ligating histidine that was modified by DEPC, His154, is in bold.

truncTfRp. The other ligating histidine, His134, was never observed to be modified by DEPC. The two nonligating histidines in truncTfRp, His120 and His162, were observed as both DEPC-modified and unmodified. As in truncTfRp, His154 was found to be modified in H120Q/H162Q, while His134 was not (Figure 5).

In addition to DEPC-modified histidines, mass shifts of +72 Da were observed for seven of the eight lysines in DEPC-treated truncTfRp and H120Q/H162Q, relative to control samples. All eight of the lysines of truncTfRp and the mutant are solvent-exposed on the large domain and are not close to the small domain containing the [2Fe-2S] cluster. One lysine, Lys95, was never found to be modified, most likely because of a crystallographically observed hydrogen bond with either Glu50 or Asp56 (PDB codes 1NYK and 3FOU) (Figure 5).

The DEPC-modified H120Q/H162Q that was treated with sodium hydroxide to remove the histidine adducts was also analyzed by mass spectrometry. Consistent with the spectroscopic data, the DEPC adduct of His154 was not observed. The lysine modifications were not affected by base treatment due to the irreversibility of the DEPC-lysine adducts and, thus, still showed the +72 Da mass shifts. Overall, the mass spectrometry results of the products from DEPC modification and reversal confirmed that ligating (His154) and nonligating histidines (His120 and His162 in truncTfRp) as well as multiple lysine residues in the large domain of truncTfRp and H120Q/H162Q were modified by DEPC (Figure 5b).

Effect of DEPC Modification on Redox State. The CD spectrum of truncTfRp or H120Q/H162Q after reaction with

DEPC for 90 min strongly resembled reduced protein. The signal loss at 340 nm, the red shift at 385 nm, and signal shift from positive to negative at 500 nm after the addition of DEPC were reminiscent of changes seen when the proteins were chemically reduced with a small excess of dithionite (Figure 6a). Since a decrease in the LMCT bands, as observed by UV-visible spectroscopy, was also seen when truncTfRp was chemically reduced, it is possible that the proteins have become reduced as a consequence of DEPC modification.

We tested the reduction hypothesis in several ways. First, the oxidant potassium ferricyanide was added to DEPC-modified H120Q/H162Q (Figure 6b). The observed shift to positive at 500 nm is consistent with the reoxidation of the [2Fe-2S] cluster of the DEPC-modified protein; however, it does not return to its initial value. This result also indicates that the [2Fe-2S] cluster remained ligated by the histidines over the course of DEPC modification and that the redox state of the protein can be manipulated with small molecules. Second, the reducing agent sodium dithionite was added to DEPC-modified protein. There was no change in the CD spectrum upon addition of the reducing agent (Figure 6c), which is consistent with the protein becoming fully reduced during the course of DEPC modification. Lastly, EPR spectra of DEPC-modified proteins (both truncTfRp and H120Q/H162Q) were acquired. This method provides the most definitive answer to the question of reduction because the oxidized [2Fe-2S] cluster of truncTfRp is EPR silent whereas the chemically reduced [2Fe-2S] cluster has an EPR signal with *g*-values at 2.03, 1.90,

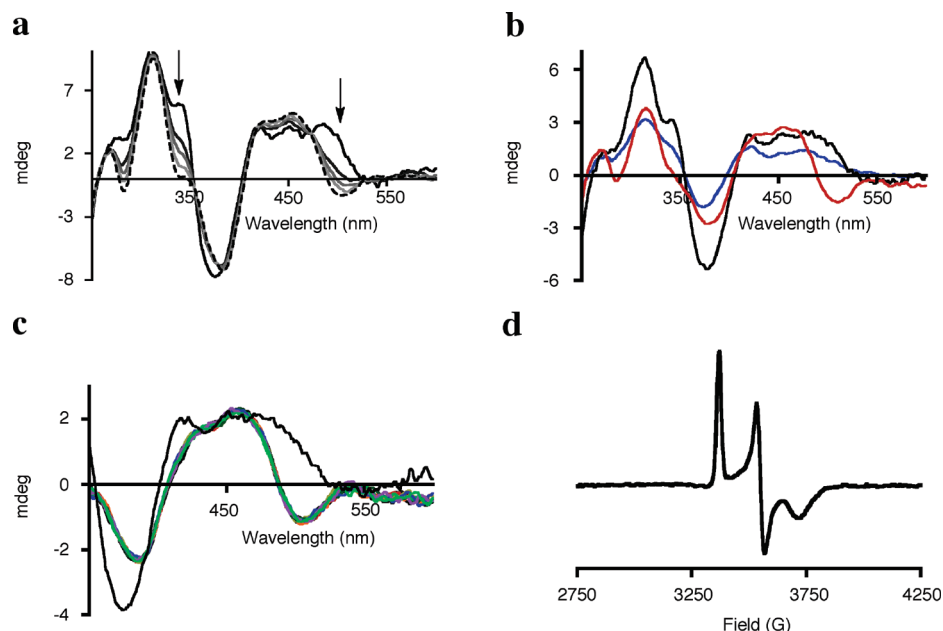


FIGURE 6: Similarity between chemically reduced and DEPC-treated H120Q/H162Q as characterized by CD. (a) H120Q/H162Q treated with a 2-fold excess of dithionite monitored every 2 min after addition. The initial spectrum is a solid black line, and the final spectrum is a dotted black line. The arrows depict the signature drops at 340 and 500 nm when the [2Fe-2S] cluster is reduced. (b) H120Q/H162Q (black line) is modified with DEPC (red line) and subsequently treated with the oxidant potassium ferricyanide (blue line). (c) H120Q/H162Q (black line) modified by DEPC (red line) and subsequently reduced with dithionite and monitored at 2 min intervals over 40 min with the final spectrum shown in green. (d) EPR spectrum of DEPC-modified H120Q/H162Q. The spectrum was collected after modification, with no added reductant. Conditions: ten scans, sweep width 2500 G, microwave power 5.02×10^{-2} , modulation amplitude 8.06 G, conversion time 41.0 ms, and RTC 81.9 ms.

and 1.80 (37). The EPR spectrum of DEPC-modified H120Q/H162Q was consistent with that of a reduced Rieske protein (Figure 6d). Addition of potassium ferricyanide to the DEPC-reduced protein completely removes the EPR signal (Supporting Information Figure S4). The g -values for both modified proteins [DEPC-trunc*Tt*Rp, (2.03, 1.90, and 1.79) and DEPC-H120Q/H162Q (2.01, 1.91, and 1.82)] were slightly shifted from the signals for chemically reduced trunc*Tt*Rp and H120Q/H162Q (Supporting Information Table S1), consistent with a small change to the cluster environment, the DEPC adduct on His154.

Effect of Redox State on DEPC Modification. The pK_a value of the reduced *Tt*Rp protein has been reported to be 12.4 (4). If the pK_a values of the protein are a measure of the histidine protonation/deprotonation, then the predominately protonated ligating histidines of the chemically reduced trunc*Tt*Rp would not be available for reaction with DEPC. H120Q/H162Q was reacted with an excess of dithionite and confirmed to be in the reduced state by CD. DEPC was added to the sample using the same protocol as above, and no change in the spectrum was observed (Figure 7a), indicating that reducing the cluster had, in fact, prevented the modification from occurring. When this sample was characterized by mass spectrometry, no modification of His154 was observed, but the lysine modifications were the same as in H120Q/H162Q that had not been “prereduced” (Figure 5b, column 4). These data are consistent with the model that the high pK_a of the ligating histidine residues in the reduced Rieske proteins from *T. thermophilus* precludes the modification of this residue by DEPC.

Potassium ferricyanide was added to H120Q/H162Q prior to the addition of DEPC, and the reaction was subsequently monitored over 90 min. The same signals (315, 340, 385, 400, 450, and 500 nm) were affected by DEPC modification in the presence or absence of an oxidant. However, the changes observed in the presence of potassium ferricyanide were of lower amplitude than

when the oxidant was not added (Figure 7b). Therefore, the DEPC-modified but oxidized (Fe(III)–Fe(III) state of [2Fe-2S] cluster) H120Q/H162Q has a significantly altered spectrum relative to the untreated protein. This is consistent with the previously discussed result that the treatment of DEPC-modified H120Q/H162Q with the oxidant does not return the spectrum to that of untreated protein. When this sample was characterized by mass spectrometry, modification of His154 and multiple lysines was seen to the same extent as in a sample of H120Q/H162Q that had not been “preoxidized” (Figure 5b, column 3). Therefore, the presence of the oxidant does not preclude modification and follows the same pattern of reaction as without the oxidant.

When H120Q/H162Q that was “preoxidized” was dialyzed after the reaction to remove excess DEPC and oxidant, and the CD spectrum was collected after dialysis, there was no color to the protein, and most of the CD signals were lost (data not shown). This indicates that the cluster is no longer incorporated in the protein under these conditions. It appears, therefore, that when forced into the oxidized state the DEPC-modified protein is unstable, in contrast to the DEPC-modified protein in the reduced state, which is stable.

DISCUSSION

Rieske proteins are electron transport metalloproteins that are central in cellular respiration. The protein’s function is to transfer an electron and a proton from quinol to cytochrome *c* (or its equivalents). As such, the molecular determinants of the pH-dependent reduction potential and their influence on interactions with small molecule inhibitors that mimic quinol are important to study.

The Rieske protein from *T. thermophilus* has two pK_a values of the oxidized protein, 7.8 and 9.6, which have been shown to originate from the deprotonation of the two ligating histidines (6, 33–37). The reported pK_{a1} and pK_{a2} values for the nitrogens in the imidazole side chain of “free histidine” are approximately 6 and 14,

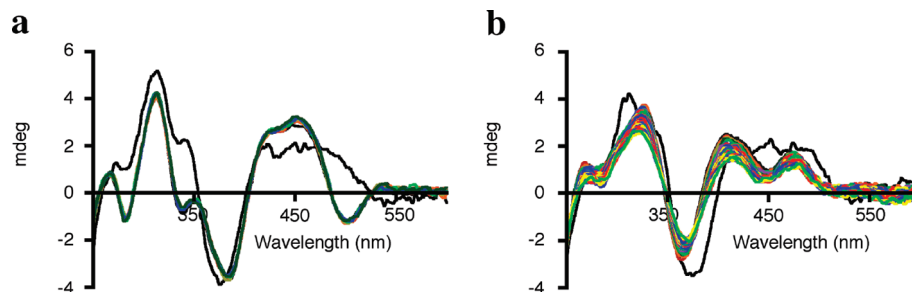


FIGURE 7: The effect on H120Q/H162Q DEPC modification by pretreatment with (a) the reductant, dithionite, and (b) the oxidant, potassium ferricyanide, monitored at 2 min intervals over 90 min after the addition of DEPC. The initial spectrum is in black, and the final spectrum is in green.

respectively. These values, however, can be altered by local protein environmental factors such as solvent accessibility, hydrogen bonding, and ligation to metal centers (38, 39). The two nonligating histidines of truncTrp, His120 and His162, are solvent exposed (Figure 1a) and should retain pK_{a1} values close to 6. The first deprotonation event is not available for the ligating histidines, His134 and His154, due to the coordinate covalent bond of N δ to the Fe atoms of the [2Fe-2S] cluster. Since the estimated pK_{a2} of histidine is 14, it is generally considered to be inaccessible in the physiological pH range. However, ligation of the histidine to the [2Fe-2S] cluster, a Lewis acid, could conceivably lower the pK_{a2} value into the pH range of 7–10 (39).

The chemical modification reagent DEPC allows for the trapping of deprotonated histidines, since only the deprotonated histidines react and form a DEPC adduct. While this reagent has been used for protein modification for over 40 years, with few exceptions (40–44), the end products of DEPC modification have not been fully characterized. The analysis of the DEPC modification of the Rieske proteins in this study was very comprehensive and included spectroscopic monitoring and definitive identification of the amino acids modified by DEPC using mass spectrometry.

UV–visible and CD spectroscopic data showed increases in reactivity of Rieske proteins with DEPC with higher pH (Figures 2 and 3), consistent with a greater concentration of deprotonated histidine ligands under these conditions. Previous work showed that the CD peak at 315 nm was responsive to changes in pH, and the changes in the signal could be plotted and fit with a single pK_a . Likewise, the signal at 340 nm was also sensitive to pH, and those changes best fit with two pK_a values (37). Therefore, it is likely that the signals at 315 and 340 nm report on the protonation/deprotonation of the histidine residues that ligate the [2Fe-2S] cluster. If so, after DEPC modification of the ligating histidine residue(s), the CD signals at both 315 and 340 nm would be affected. Indeed, both were observed to change after reaction with DEPC. The change at 315 nm occurred on the same time scale as the accumulation of the 250 nm chromophore, as seen by UV–visible spectroscopy, indicating a relationship between formation of the adduct on His154 and the change at 315 nm. Elevation of pH increased the amount of change seen at these wavelengths (Figure 3). All of the spectroscopic data are, therefore, consistent with a model in which DEPC is reacting with and modifying a deprotonated ligating histidine residue as shown schematically in Figure 8.

Mass spectrometry results indicated that one ligating histidine, His154, was modified by DEPC, but His134, the other histidine ligand to the [2Fe-2S] cluster, was never detected in the modified state (Figure 5b). The accessibility and reactivity of His154 to

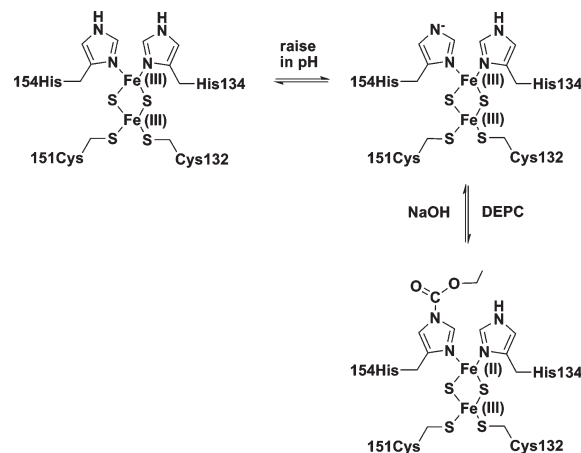


FIGURE 8: Model of DEPC modification of ligating histidine His154 of the Rieske protein from *T. thermophilus*. As the pH is raised, His154 becomes deprotonated, allowing reaction with DEPC. The formation of the carbethoxy–histidine adduct on His154 subsequently induces a one-electron reduction of the [2Fe-2S] cluster from Fe(III)–Fe(III) to Fe(II)–Fe(III).

covalent modification by DEPC are consistent with His154 having the lower pK_a (6). Additionally, this covalent modification may mimic the hydrogen bond interactions observed in cocrystal structures made between the His154 equivalent in the bovine or *Rhodobacter sphaeroides* bc_1 complex and small molecules such as stigmatellin. Among these cocrystal structures, the histidine equivalent to His154 is always the residue that is hydrogen bonded to the small molecule, while the His134 equivalent does not interact (14–16, 18, 21, 22, 24). The reactivity of His154 and the inaccessibility of His134 to DEPC modification in solution closely parallel the interactions seen in the cocrystal structures.

The modification of His154, and not His134, by DEPC is consistent with and independently confirms the finding that the lower pK_a corresponds with His154 (6). His134 is sterically restricted by Leu135. Interestingly, this leucine ($n + 1$ of the lower numbered ligating histidine) is conserved among the respiratory-type Rieske proteins (1, 3). In fact, preliminary studies of DEPC modification of a mutant of truncTrp, L135A, in which the bulky side chain of leucine is eliminated, can be modified at both His154 and His134 (data not shown). Thus, His154 is the first to deprotonate, and there is conserved steric hindrance for His134 that precludes reaction with the DEPC molecule.

Another important consideration is that the mass spectrometry analysis shows multiple lysine modifications as well as histidine modifications. The overall effect of these modifications is unclear. However, once the adduct from His154 is removed using high pH (Figure 4a), the CD spectrum is identical to untreated

protein at an equivalent pH. These data indicate that the lysine modifications do not affect the CD spectrum in the visible wavelengths appreciably. Thus, the changes observed in the visible region with DEPC modification are due to alteration of the ligating histidines and not due to the modification of lysines.

In myoglobin, modification of one of the ligating histidines (His97) by high concentrations of DEPC resulted in loss of the heme cofactor (40). However, in the case of cytochrome *b*₅₆₁, modification of the heme-ligating histidine by DEPC did not disrupt the coordinate-covalent bond of the heme iron to the N δ of the modified histidine (45–48). In our study, reaction of trunc*T*rRp and H120Q/H162Q with DEPC resulted in modification of the ligating histidine His154 and alteration of the reduction potential and the spectral signals originating from the [2Fe-2S] cluster but did not weaken the coordinate-covalent bond such that the cluster was lost. In previous work, addition of DEPC to the complete *bc*₁ complex inhibited activity. The authors suggested that modification of histidines was responsible, but they did not elucidate the mechanism for this inhibition (10–12). The results presented here confirm that the addition of the carbethoxy functional group to a ligating histidine residue causes reduction of the [2Fe-2S] cluster, which would stop the Rieske protein from gaining an electron from quinol within the larger *bc*₁ complex, thus inhibiting the complex.

Inhibition of the *bc*₁ complex by stigmatellin, chromonols, and ascochlorin has been postulated to be, at least in part, through interaction with a ligating histidine of the Rieske protein (30–32). Previous work showed that when stigmatellin was added to the bovine *bc*₁ complex, there was an increase in reduction potential from +290 to +540 mV (29). Stigmatellin has also been recently shown to reduce the [2Fe-2S] cluster of the Rieske protein in the bovine *bc*₁ complex (30). Like the reduction caused by stigmatellin, the source of the electron for the DEPC-induced reduction is unknown. In order for the observed DEPC-induced reduction of the proteins in our study to take place, the reduction potential must increase as a consequence of modification, analogous to the effects of stigmatellin, though no covalent bond is formed as a consequence of treatment with this inhibitor. Therefore, the DEPC adduct of His154 that ligates the [2Fe-2S] cluster in trunc*T*rRp and H120Q/H162Q models the possible mechanism of inhibition by stigmatellin and related compounds.

In summary, the reaction of trunc*T*rRp and H120Q/H162Q with DEPC at various pH values results in modification of His154 as well as multiple lysine residues in the large domain. The formation of the ligand histidine adduct traps the deprotonated histidine, and it is detected at pH 7.6 by mass spectrometry. The reduction of the [2Fe-2S] cluster as a result of DEPC modification models the interaction of Rieske proteins with small molecule inhibitors of the mitochondrial *bc*₁ complex such as stigmatellin. Chemical modification by DEPC offers a way to study the reactivity and accessibility of the ligating histidine residues and probes the influence of these histidines on the redox properties of the Rieske protein.

ACKNOWLEDGMENT

We acknowledge Dr. David Britt, Jamie Stull, and Emily Ricks of the University of California at Davis for collecting and processing the EPR data. Nick Karagas is also acknowledged for preparing some control experiments. We also thank Drs. Bert Chandler and Adam Urbach for helpful discussions. Sequencing was performed at the Nucleic Acids Core Facility at the University

of Texas Health Science Center at San Antonio. Mass spectrometry analyses were conducted in the Institutional Mass Spectrometry Laboratory at the University of Texas Health Science Center at San Antonio.

SUPPORTING INFORMATION AVAILABLE

Comparison between trunc*T*rRp and H120Q/H162Q by CD, the pH titration of H120Q/H162Q, the pH-dependent DEPC modification of trunc*T*rRp using CD, and a table of *g*-values for modified and chemically reduced trunc*T*rRp and H120Q/H162Q. This material is available free of charge via the Internet at <http://pubs.acs.org>.

REFERENCES

- Link, T. A. (1999) The Structures of Rieske and Rieske-Type Proteins. *Adv. Inorg. Chem.* 47, 83–157.
- Berry, E. A., Guergova-Kuras, M., Huang, L. S., and Crofts, A. R. (2000) Structure and Function of Cytochrome *bc* Complexes. *Annu. Rev. Biochem.* 69, 1005–1075.
- Hunsicker-Wang, L. M., Heine, A., Chen, Y., Luna, E. P., Todaro, T., Zhang, Y., Williams, P. A., McRee, D. E., Hirst, J., Stout, C. D., and Fee, J. A. (2003) High Resolution Structure of the Soluble, Respiratory-Type Rieske Protein from *Thermus thermophilus*: Analysis and Comparison. *Biochemistry* 42, 7303–7317.
- Zu, Y., Fee, J. A., and Hirst, J. (2001) Complete Thermodynamic Characterization of Reduction and Protonation of the *bc*₁-Type Rieske [2Fe-2S] Center of *Thermus thermophilus*. *J. Am. Chem. Soc.* 123, 9906–9907.
- Zu, Y., Couture, M. M., Kolling, D. R. J., Crofts, A. R., Eltis, L. D., Fee, J. A., and Hirst, J. (2003) Reduction Potentials of Rieske Clusters: Importance of the Coupling between Oxidation State and Histidine Protonation State. *Biochemistry* 42, 12400–12408.
- Hsueh, K., Westler, W. M., and Markley, J. L. (2010) NMR Investigations of the Rieske Protein from *Thermus thermophilus* Support a Coupled Proton and Electron Transfer Mechanism. *J. Am. Chem. Soc.* 132, 7908–7918.
- Miles, E. W. (1977) Modification of Histidyl Residues in Proteins by Diethylpyrocarbonate. *Methods Enzymol.* 47, 431–442.
- Lundblad, R. L. (2005) Chemical Reagents for Protein Modification, 3rd ed., pp 73–87, CRC Press, Boca Raton, FL.
- Yagi, T., Vik, S. B., and Hatefi, Y. (1982) Reversible Inhibition of the Mitochondrial Ubiquinol-Cytochrome *c* Oxidoreductase Complex (Complex III) by Ethoxyformic Anhydride. *Biochemistry* 21, 4777–4782.
- Ohnishi, T., Meinhardt, S. W., von Jagow, G., Yagi, T., and Hatefi, Y. (1994) Effect of Ethoxyformic Anhydride on the Rieske Iron-Sulfur Protein of Bovine Heart Ubiquinol: Cytochrome *c* Oxidoreductase. *FEBS Lett.* 353, 103–107.
- Lorusso, M., Gatti, D., Boffoli, D., Bellomo, E., and Papa, S. (1983) Redox-Linked Proton Translocation in the *bc*₁ Complex from Beef-Heart Mitochondria Reconstituted into Phospholipid Vesicles. Studies with Chemical Modifiers of Amino Acid Residues. *Eur. J. Biochem.* 137, 413–420.
- Lorusso, M., Gatti, D., Marzo, M., Boffoli, D., Cocco, T., and Papa, S. (1987) Chemical Modification Studies of Beef-Heart Mitochondrial *bc*₁ Complex. Effect of Modification by Ethoxyformic Anhydride. *Eur. J. Biochem.* 162, 231–238.
- Zhang, Z., Huang, L., Shulmeister, V. M., Chi, Y. I., Kim, K. K., Hung, L. W., Crofts, A. R., Berry, E. A., and Kim, S. H. (1998) Electron Transfer by Domain Movement in Cytochrome *bc*₁. *Nature* 392, 677–684.
- Berry, E. A., Huang, L. S., Saechao, L. K., Pon, N. G., Valkova-Valchanova, M., and Daldal, F. (2004) X-Ray Structure of *Rhodobacter capsulatus* Cytochrome *bc*(1): Comparison with its Mitochondrial and Chloroplast Counterparts. *Photosynth. Res.* 81, 251–275.
- Esser, L., Elberry, M., Zhou, F., Yu, C. A., Yu, L., and Xia, D. (2008) Inhibitor-Complexed Structures of the Cytochrome *bc*₁ from the Photosynthetic Bacterium *Rhodobacter sphaeroides*. *J. Biol. Chem.* 283, 2846–2857.
- Esser, L., Quinn, B., Li, Y. F., Zhang, M., Elberry, M., Yu, L., Yu, C. A., and Xia, D. (2004) Crystallographic Studies of Quinol Oxidation Site Inhibitors: A Modified Classification of Inhibitors for the Cytochrome *bc*(1) Complex. *J. Mol. Biol.* 341, 281–302.

17. Esser, L., Gong, X., Yang, S., Yu, L., Yu, C. A., and Xia, D. (2006) Surface-Modulated Motion Switch: Capture and Release of Iron-Sulfur Protein in the Cytochrome *bc*₁ Complex. *Proc. Natl. Acad. Sci. U.S.A.* 103, 13045–13050.
18. Gao, X., Wen, X., Esser, L., Quinn, B., Yu, L., Yu, C. A., and Xia, D. (2003) Structural Basis for the Quinone Reduction in the *bc*₁ complex: A Comparative Analysis of Crystal Structures of Mitochondrial Cytochrome *bc*₁ with Bound Substrate and Inhibitors at the Q_i Site. *Biochemistry* 42, 9067–9080.
19. Gao, X., Wen, X., Yu, C., Esser, L., Tsao, S., Quinn, B., Zhang, L., Yu, L., and Xia, D. (2002) The Crystal Structure of Mitochondrial Cytochrome *bc*₁ in Complex with Famoxadone: The Role of Aromatic-Aromatic Interaction in Inhibition. *Biochemistry* 41, 11692–11702.
20. Crowley, P. J., Berry, E. A., Cromartie, T., Daldal, F., Godfrey, C. R., Lee, D. W., Phillips, J. E., Taylor, A., and Viner, R. (2008) The Role of Molecular Modeling in the Design of Analogues of the Fungicidal Natural Products Crocacin A and D. *Bioorg. Med. Chem.* 16, 10345–10355.
21. Huang, L. S., Cobessi, D., Tung, E. Y., and Berry, E. A. (2005) Binding of the Respiratory Chain Inhibitor Antimycin to the Mitochondrial *bc*₁ Complex: A New Crystal Structure Reveals an Altered Intramolecular Hydrogen-Bonding Pattern. *J. Mol. Biol.* 351, 573–597.
22. Lancaster, C. R., Hunte, C., Kelley, J., 3rd, Trumpower, B. L., and Ditchfield, R. (2007) A Comparison of Stigmatellin Conformations, Free and Bound to the Photosynthetic Reaction Center and the Cytochrome *bc*₁ Complex. *J. Mol. Biol.* 368, 197–208.
23. Hunte, C., Koepke, J., Lange, C., Rossmanith, T., and Michel, H. (2000) Structure at 2.3 Å Resolution of the Cytochrome *bc*₁ Complex from the Yeast *Saccharomyces cerevisiae* Co-Crystallized with an Antibody F_v Fragment. *Structure* 8, 669–684.
24. Lange, C., and Hunte, C. (2002) Crystal Structure of the Yeast Cytochrome *bc*₁ Complex with its Bound Substrate Cytochrome *c*. *Proc. Natl. Acad. Sci. U.S.A.* 99, 2800–2805.
25. Lange, C., Nett, J. H., Trumpower, B. L., and Hunte, C. (2001) Specific Roles of Protein-Phospholipid Interactions in the Yeast Cytochrome *bc*₁ Complex Structure. *EMBO J.* 20, 6591–6600.
26. Palsdottir, H., Lojero, C. G., Trumpower, B. L., and Hunte, C. (2003) Structure of the Yeast Cytochrome *bc*₁ Complex with a Hydroxyquinone Anion Q_o Site Inhibitor Bound. *J. Biol. Chem.* 278, 31303–31311.
27. Solmaz, S. R., and Hunte, C. (2008) Structure of Complex III with Bound Cytochrome *c* in Reduced State and Definition of a Minimal Core Interface for Electron Transfer. *J. Biol. Chem.* 283, 17542–17549.
28. Xia, D., Yu, C. A., Kim, H., Xia, J. Z., Kachurin, A. M., Zhang, L., Yu, L., and Deisenhofer, J. (1997) Crystal Structure of the Cytochrome *bc*₁ Complex from Bovine Heart Mitochondria. *Science* 277, 60–66.
29. von Jagow, G., and Ohnishi, T. (1985) The Chromone Inhibitor Stigmatellin—Binding to the Ubiquinol Oxidation Center at the C-Side of the Mitochondrial Membrane. *FEBS Lett.* 185, 311–315.
30. Gurung, B., Yu, L., and Yu, C. A. (2008) Stigmatellin Induces Reduction of Iron-Sulfur Protein in the Oxidized Cytochrome *bc*₁ Complex. *J. Biol. Chem.* 283, 28087–28094.
31. Berry, E. A., Huang, L. S., Lee, D. W., Daldal, F., Nagai, K., and Minagawa, N. (2010) Ascochlorin is a Novel, Specific Inhibitor of the Mitochondrial Cytochrome *bc*₁ Complex. *Biochim. Biophys. Acta* 1797, 360–370.
32. Mullebnner, A., Patel, A., Stamberg, W., Staniek, K., Rosenau, T., Netscher, T., and Gille, L. (2010) Modulation of the Mitochondrial Cytochrome *bc*₁ Complex Activity by Chromanols and Related Compounds. *Chem. Res. Toxicol.* 23, 193–202.
33. Lin, I., Chen, Y., Fee, J. A., Song, J., Westler, W. M., and Markley, J. L. (2006) Rieske Protein from *Thermus thermophilus*: ¹⁵N NMR Titration Study Demonstrates the Role of Iron-Ligated Histidines in the pH Dependence of the Reduction Potential. *J. Am. Chem. Soc.* 128, 10672–10673.
34. Kuila, D., Schoonover, J. R., Dyer, R. B., Batie, C. J., Ballou, D. P., Fee, J. A., and Woodruff, W. H. (1992) Resonance Raman Studies of Rieske-Type Proteins. *Biochim. Biophys. Acta* 1140, 175–183.
35. Iwaki, M., Yakovlev, G., Hirst, J., Osyczka, A., Dutton, P. L., Marshall, D., and Rich, P. R. (2005) Direct Observation of Redox-Linked Histidine Protonation Changes in the Iron-Sulfur Protein of the Cytochrome *bc*₁ Complex by ATR-FTIR Spectroscopy. *Biochemistry* 44, 4230–4237.
36. Ullmann, G. M., Noodleman, L., and Case, D. A. (2002) Density Functional Calculation of pK_a Values and Redox Potentials in the Bovine Rieske Iron-Sulfur Protein. *J. Biol. Inorg. Chem.* 7, 632–639.
37. Konkle, M. E., Muellner, S. K., Schwander, A. L., Dicus, M. M., Pokhrel, R., Britt, R. D., Taylor, A. B., and Hunsicker-Wang, L. M. (2009) Effect of pH on the Rieske Protein from *Thermus thermophilus*: A Spectroscopic and Structural Analysis. *Biochemistry* 48, 9848–9857.
38. Altman, J., Lipka, J. J., Kuntz, I., and Waskell, L. (1989) Identification by Proton Nuclear Magnetic Resonance of the Histidines in Cytochrome *b*₅ Modified by Diethyl Pyrocarbonate. *Biochemistry* 28, 7516–7523.
39. George, P., Hanania, G. I. H., Irvine, D. H., and Asu-Issa, I. (1964) Effect of Coordination on Ionization. Part IV. Imidazole and its Ferrimyoglobin Complex. *J. Chem. Soc.*, 5689–5694.
40. Nakanishi, N., Takeuchi, F., Park, S., Hori, H., Kivota, K., Uno, T., and Tsubaki, M. (2008) Characterization of Heme-Coordinating Histidyl Residues of an Engineered Six-Coordinated Myoglobin Mutant Based on the Reactivity with Diethylpyrocarbonate, Mass Spectrometry, and Electron Paramagnetic Resonance Spectroscopy. *J. Biosci. Bioeng.* 105, 604–613.
41. Narindrasorasak, S., Kulkarni, P., Deschamps, P., She, Y. M., and Sarkar, B. (2007) Characterization and Copper Binding Properties of Human COMMD1 (MURR1). *Biochemistry* 46, 3116–3128.
42. Jin, X. R., Abe, Y., Li, C. Y., and Hamasaki, N. (2003) Histidine-834 of Human Erythrocyte Band 3 has an Essential Role in the Conformational Changes that Occur during the Band 3-Mediated Anion Exchange. *Biochemistry* 42, 12927–12932.
43. Hondal, R. J., Ma, S., Caprioli, R. M., Hill, K. E., and Burk, R. F. (2001) Heparin-Binding Histidine and Lysine Residues of Rat Selenoprotein P. *J. Biol. Chem.* 276, 15823–15831.
44. Dage, J. L., Sun, H., and Halsall, H. B. (1998) Determination of Diethylpyrocarbonate-Modified Amino Acid Residues in Alpha 1-Acid Glycoprotein by High-Performance Liquid Chromatography Electrospray Ionization-Mass Spectrometry and Matrix-Assisted Laser desorption/ionization Time-of-Flight-Mass Spectrometry. *Anal. Biochem.* 257, 176–185.
45. Tsubaki, M., Kobayashi, K., Ichise, T., Takeuchi, F., and Tagawa, S. (2000) Diethyl Pyrocarbonate Modification Abolishes Fast Electron Accepting Ability of Cytochrome *b*₅₆₁ from Ascorbate but does Not Influence Electron Donation to Monodehydroascorbate Radical: Identification of the Modification Sites by Mass Spectrometric Analysis. *Biochemistry* 39, 3276–3284.
46. Nakanishi, N., Rahman, M. M., Sakamoto, Y., Miura, M., Takeuchi, F., Park, S., and Tsubaki, M. (2009) Inhibition of Electron Acceptance from Ascorbate by the Specific N-Carboxylations of Maize Cytochrome *b*₅₆₁: A Common Mechanism for the Transmembrane Electron Transfer in Cytochrome *b*₅₆₁ Protein Family. *J. Biochem.* 146, 587–586.
47. Kipp, B. H., Kelley, P. M., and Njus, D. (2001) Evidence for an Essential Histidine Residue in the Ascorbate-Binding Site of Cytochrome *b*₅₆₁. *Biochemistry* 40, 3931–3937.
48. Takeuchi, F., Kobayashi, K., Tagawa, S., and Tsubaki, M. (2001) Ascorbate Inhibits the Carbethoxylation of Two Histidyl and One Tyrosyl Residues Indispensable for the Transmembrane Electron Transfer Reaction of Cytochrome *b*₅₆₁. *Biochemistry* 40, 4067–4076.